Advances in Environmental Technology 3 (2021) 185-194

Iranian Reasearch Organization for Science and Technology (IROST)

Advances in Environmental Technology

Journal home page: https://aet.irost.ir/

Factors affecting photocatalytic degradation of Reactive Green-19 with CdO-TiO_2 nanocomposite

Gaurav Zope[1], Ajaygiri Goswami[1], Sunil Kulkarni[2*], Pawan Meshram[1]

[1]University Institute of Chemical Technology, Kavayitri Bahinabai Chaudhari North Maharashtra University, Jalgaon, Maharashtra, India

[2]Gharda Institute of Technology, Lavel. Maharashtra, India

ARTICLE INFO

Article history:
Received 1 October 2021
Received in revised form
20 December 2021
Accepted 22 December 2021

Keywords:
Precursors
XRD
Peaks
Light intensity
Morphology
Chemical stability

ABSTRACT

Cdo-TiO_2 nanocomposites were synthesized by varying the molar ratio of CdO: TiO_2 as 1:1, 1:2, and 2:1 using the sol-gel method. The pH value for all the CdO-TiO_2 nanocomposites was controlled at two different values, pH-3 and pH-13. The nanocomposites were used for facilitating photolytic degradation of azo dye (Reactive Green-19). The surface morphology, crystallinity, and properties related to interactions with the light of the prepared catalyst were examined by scanning electron microscopy (FE-SEM), X-ray diffraction (XRD), and ultraviolet-visible (UV-Vis) spectrophotometer, respectively. The nanocomposites for all molar ratios synthesized at pH-3 showed rod-like structure and some irregular shapes, while those synthesized at pH-13 were spherical. From XRD patterns, composites at pH-3 and pH-13 were crystalline; however, those at pH-3 were more crystalline. The parameters, namely initial dye concentration, pH of dye solution, and catalyst concentration, affecting photocatalytic activities were examined and optimized at 75 ppm, pH-7.5, and 1g/L, respectively. The progress of the degradation process of Reactive Green-19 was observed by monitoring the change in the concentration of the dye after a certain time interval by measuring the absorbance by UV-Vis spectrophotometer. Catalyst A1:1 (The nanocomposites obtained at pH-3 with 1:1 mol% of CdO:TiO_2) showed maximum degradation (94.53 %) at a catalyst concentration of 1 g/L.

1. Introduction

Sustainable growth is the most important aspect of modern-day research. Rapid industrialization and simultaneous increase in environmental concern have attracted the attention of many researchers towards wastewater treatment. Textile industry effluent is one of the significant sources of water pollution in India. This effluent contains mainly organic dyes and compounds. These compounds can cause diseases such as cancer. Other harmful effects of this effluent include mutagenicity, skin irritation, and ulceration of the skin [1,2].

*Corresponding author:
E-mail: suniljayantkulkarni@gmail.com
DOI: 10.22104/AET.2021.5140.1395

Worldwide, textile industries use azo dyes, a significant class of synthetic dyes, because of their low cost and availability in various color variants [3]. The presence of one or more aromatic parts with azo bonds (-N=N-) is characterized as reactive dyes [4]. The most common colorant widely used in textiles, paint, and garment industries is reactive Green 19(RG-19). RG- 19 molecular structure has twin azo groups as a chromophoric moiety. Also, it has a couple of reactive chlorotriazine groups. The presence of these reactive groups makes Reactive Green 19 the most preferred azo dye in textile industries. [5]. When applied to fabric, it gets washed away with water, generating a huge amount of effluent that needs to be treated. These azo dyes cause health problems for humans and animals if they enter the body through drinking water. The effluent containing azo dyes needs to be treated for degrading the dyes before it is discharged into the environment. Advanced oxidation processes (AOPs) are universally recognized nowadays for the complete destruction of contaminants present in wastewater. Adsorption [6,7], chemical oxidation [8], electro-coagulation [9], microbial action [10,11], and photocatalysis [12,13] are various AOPs that are generally used for wastewater treatment; each process has its own limitations. Nowadays, most studies have focused on photocatalysis using semiconducting nanomaterials as the catalyst for the degradation of reactive azo dyes. Heterogenous photocatalysis has emerged as an important process for removing organic pollutants that are soluble in water [14-16]. For the complete destruction of organic pollutants, various types of semiconductors like titanium dioxide, zinc oxide, cadmium sulfide, tungsten trioxide are widely used in the photocatalytic process [17-19]. As per the literature, TiO_2 is one of the most frequently used photocatalyst due to its photosensitive and stable nature. [17-20]. Semiconductor nanoparticles with different band gaps are coupled to increase the efficiency of the photocatalytic process [21,22]. Recently, CdO (2.2 eV) has been reported as an important semiconductor for the wastewater treatment of organic pollutants [23]. CdO- TiO_2 nanocomposites have been used for the degradation of organic methyl blue and methyl orange dyes with 99 and 97 percent degradation efficiency, respectively [24]. The objective of the present work is to synthesize and characterize CdO/TiO_2 nanoparticles and study their use in the photolytic degradation of Reactive Green 19 (RG-19) dye. The optimum proportion of CdO and TiO_2 is determined by carrying out experiments at different proportions based on earlier reported results. In the present investigation, the synthesis of CdO/TiO_2 nanocomposite is carried out at different CdO/TiO_2 molar ratios (1:1, 1:2 and 2:1) and pH values (3 and 13) using cadmium acetate and titanium isopropoxide (TTIP) as precursors of CdO and TiO_2. The effect of different molar ratios and pH on surface morphology, crystallinity, and band gap of nanocomposite was determined using FE-SEM, XRD, and UV-spectrophotometer, respectively. The prepared CdO/TiO_2 nanocomposites were used for the light-induced decomposition of Reactive Green 19 (RG-19). The influence of parameters like initial dye composition, the concentration of catalyst, and pH of dye solution were examined.

2. Materials and methods

2.1. Materials

TTIP and cadmium acetate were procured from Avra Chemicals (Hyderabad, India). The ethanol was procured from Merck, Germany. The hydrochloric acid and liquid ammonia were purchased from Merck, India. The Reactive Green-19 dye was purchased from Sigma Aldrich.

2.2. Synthesis of CdO/TiO_2 nanoparticles

The nano-sized CdO-TiO_2 was formed by a simple sol-gel technique using cadmium acetate and TTIP as precursors of CdO and TiO2, respectively. The precursors of cadmium acetate and TTIP (1:1 mol %) were separately hydrolyzed at 80 °C in distilled water. The pH (acidic-3, basic-13) of both precursors were adjusted by using 0.1N each of HCl and liquid ammonia. Then, both precursor solutions were mixed and agitated for 10 minutes. Subsequently, 50 ml of distilled water was added to the mixture and stirred. After 30 minutes, the required pH of the overall reaction was again maintained, and vigorous agitation was carried out at 80°C for three hours. The obtained solution was dried in a hot air oven at 100 °C until completely dry. Calcination was performed at 450 °C for 180

minutes in a muffle furnace to increase the crystallinity of the nanoparticles. The nanocomposites obtained at pH-3 and pH-13 were named A1:1 and B1:1, respectively. The same procedure was repeated for 1:2 and 2:1 mol% of CdO: TiO2 nanocomposites for both pHs and named A1:2, B1:2 and A2:1, B2:1, respectively. This proportion was estimated based on the findings of an earlier investigation [24].

2.3. Characterization methods

Scanning electron microscopy (FE-SEM-S 4800, Hitachi, Japan) was used for determining the shape, size, and surface characteristics. The study of the size, shape, and structure of the nanocomposites was carried out by facilitating the golden layer using an ion sputter (Hitachi E1010). For this purpose, the nanocomposite was fitted on a brass stub with adhesive tape at 5 pascal pressure in an ion sputter (Hitachi E1010). XRD using a (Bruker AXS D8 Advance) diffractometer was employed for structural analysis. The XRD patterns were obtained over the angular range of 2θ = 10 – 80°. The optical properties of the nanocomposites were studied for the calculation of band gap energy with a Double Beam UV 1800 spectrophotometer (Shimadzu, Tokyo, Japan) in the 200-800 nanometer range. The synthesized nanoparticles (1g/cc) were dispersed in ethanol with an ultrasonic probe sonicator(Athena-ATP-150) for 15 minutes prior to recording.

2.4. Experimental procedure for light induced degradation of dyes

The degradation of the RG-19 was conducted for all synthesized catalysts at a different pH and molar ratio. A simple batch reactor under solar light irradiation was used for this examination. An Illumination Digital Lux Meter (TES-1332A) was used to measure solar intensity. The experiments were scheduled between 11 am to 4 pm IST to ensure a sufficient intensity of light. In Jalgaon, the summer temperature is 33 ^{0}C, and the average light intensity is 130 Lumens per square meter. Experiments were conducted in a 250 ml beaker as the batch reactor. In each experiment, solutions at different concentrations of RG-19 dye (50, 75, and 100 ppm) were prepared; different concentrations of synthesized CdO-TiO_2 nanocomposites (0.5, 1, and 1.5 gm/lit) were added to the dye solutions, and these were placed on the magnetic stirrer under solar irradiation. The pH of the dye solution was maintained by adding 0.1 N hydrochloric acid and 0.1 N sodium hydroxide. The photocatalytic degradation progress of RG-19 was monitored. For this, aliquot samples were withdrawn at regular time intervals. These aliquots were filtered using a syringe filter, and the absorbance spectra were recorded in a UV-Vis spectrophotometer.

3. Results and discussion

3.1. Field emission scanning electron microscope analysis (FE-SEM)

The surface morphology of the synthesized CdO-TiO_2 nanocomposites at pH-3 and pH-13 with a different molar ratio of the precursor is shown in Figure 1. For the equal concentration of CdO and TiO_2, the composite consisted of nanorods with an approximate diameter of 80-90 nm and were aligned randomly. The composite A1:2 contained nanorods that were aggregated, but A 2:1 was comprised of nanorods with few polygon-shaped structures. B1:1, B1:2, and B2:1were prepared at pH-13, and the effect of the pH change was clearly seen due to the change in morphology from nanorods to spherical particles. The B1:1 composite was observed as an aggregated sphere with an average diameter equal to 70-75 nm; the B1:2 composites appeared like spheres bound in the shape of a tripod. These nanocomposites also possessed some hexagonal structure. The B2:1 composite was aggregated to form a secondary spherical structure with relatively large size-like corals.

3.2. X-Ray Diffraction Analysis (XRD)

The XRD pattern of all the synthesized CdO-TiO_2 nanocomposites at various molar ratios of CdO: TiO_2 and at different pH values (pH-3 and pH-13) are depicted in Figures 2(A) and 2(B). A comparison with the standard database of CdO and TiO_2 indicates that the peaks of both compounds are present in diffraction patterns. The characteristic peaks of TiO_2 at angles 25.3^0, 37.8^0, 46.1^0, 53.9^0, 58.0^0, 62.7^0, and 68.8^0 corresponds to the respective (101), (112), (-531), (105), (204), (213), and (116) diffraction peaks of anatase phase TiO_2 according to the reference patterns by the Joint Committee on Powder

Diffraction (JCPDS 898-4921). The CdO peaks at angles 30.0^0, 33.2^0, 38.33^0, 49.9^0, and 56.00 correspond to the (100), (111), (200), (110), and (220) planes, respectively, which resembles the cubic structure of CdO as per reference patterns (JCPDS card no. 65-2908). A small alteration in the intensity of the peaks was seen due to variation in the molar ratio of CdO and TiO_2. The intensity of the peaks was lower at pH-3 than pH-13, which indicated that at pH-3, the material was more crystalline than at pH-13. Also, it was observed that some peaks were absent at pH-13, i.e., 2θ = 25.3^0, 53.9^0, 56.0^0, 62.7^0, and 68.8^0.

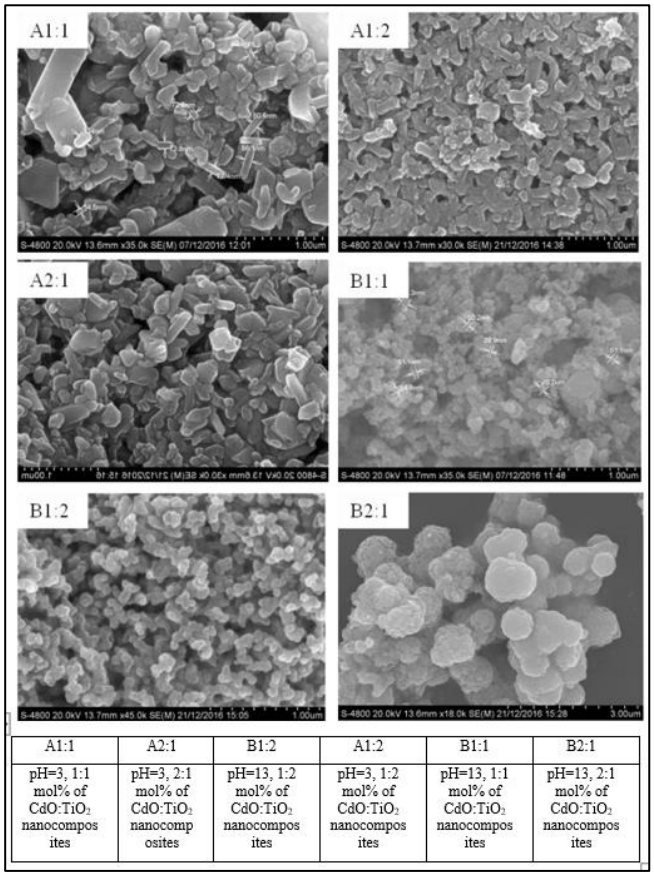

A1:1	A2:1	B1:2	A1:2	B1:1	B2:1
pH=3, 1:1 mol% of $CdO:TiO_2$ nanocompos ites	pH=3, 2:1 mol% of $CdO:TiO_2$ nanocomp ositeS	pH=13, 1:2 mol% of $CdO:TiO_2$ nanocompos ites	pH=3, 1:2 mol% of $CdO:TiO_2$ nanocompos ites	pH=13, 1:1 mol% of $CdO:TiO_2$ nanocompos ites	pH=13, 2:1 mol% of $CdO:TiO_2$ nanocompos ites

Fig.1. Surface morphology with different molar ratio of precursor.

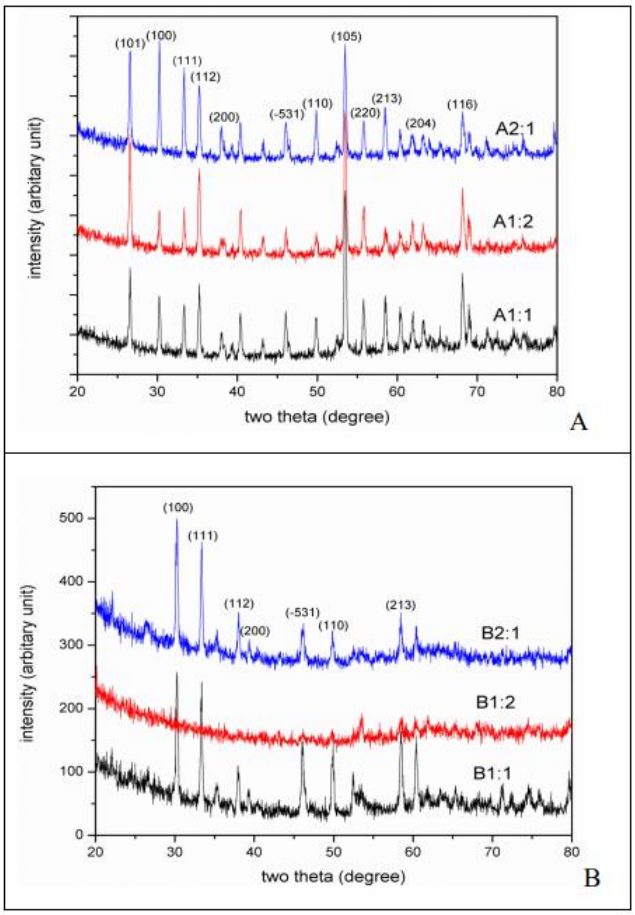

Fig. 2. XRD pattern of Synthesized catalyst [A. at pH=3, B.At pH=13].

3.3. UV-Vis spectrophotometer

The UV-Vis spectra for all synthesized photocatalysts are shown in Fig. 3. The absorbance versus wavelength plots for the above six combinations (A1:1 to B2:1) are plotted in this figure. The CdO-TiO_2 ratio has a significant effect on absorbance-wavelength characteristics.

3.4. Effect of initial dye composition

The effect of initial dye content ($C_{0)}$ on the process of decomposition of RG-19 by CdO-TiO_2 is studied experimentally. The runs were carried out with different concentrations of RG-19 [50 ppm, 75 ppm, and 100 ppm]. The catalyst concentration was maintained at 1 g/L, and the pH of the solution (7.5) was kept constant. The results are shown in Figure 4. It is seen that at a higher concentration of RG-19, the percentage degradation was less. A high concentration of dye results in a deep-colored solution that decreases UV light penetration. When the concentration of RG-19 increased, the equilibrium adsorption of dye on the CdO-TiO_2 catalyst also increased, which reduced the adsorption of the hydroxyl radical (*OH), an active species for photocatalytic degradation [25]. So, when C_0 increased, the rate

of photocatalytic degradation of RG-19 decreased. From Figure 4, we can conclude that the photocatalysts of A1:1 (92.38 %) and B2:1 (92.30 %) show maximum degradation of dye for the C_0 value of 75 ppm and 50 ppm, respectively, after 160 min. Hence, 75 ppm was taken as the optimum initial dye concentration.

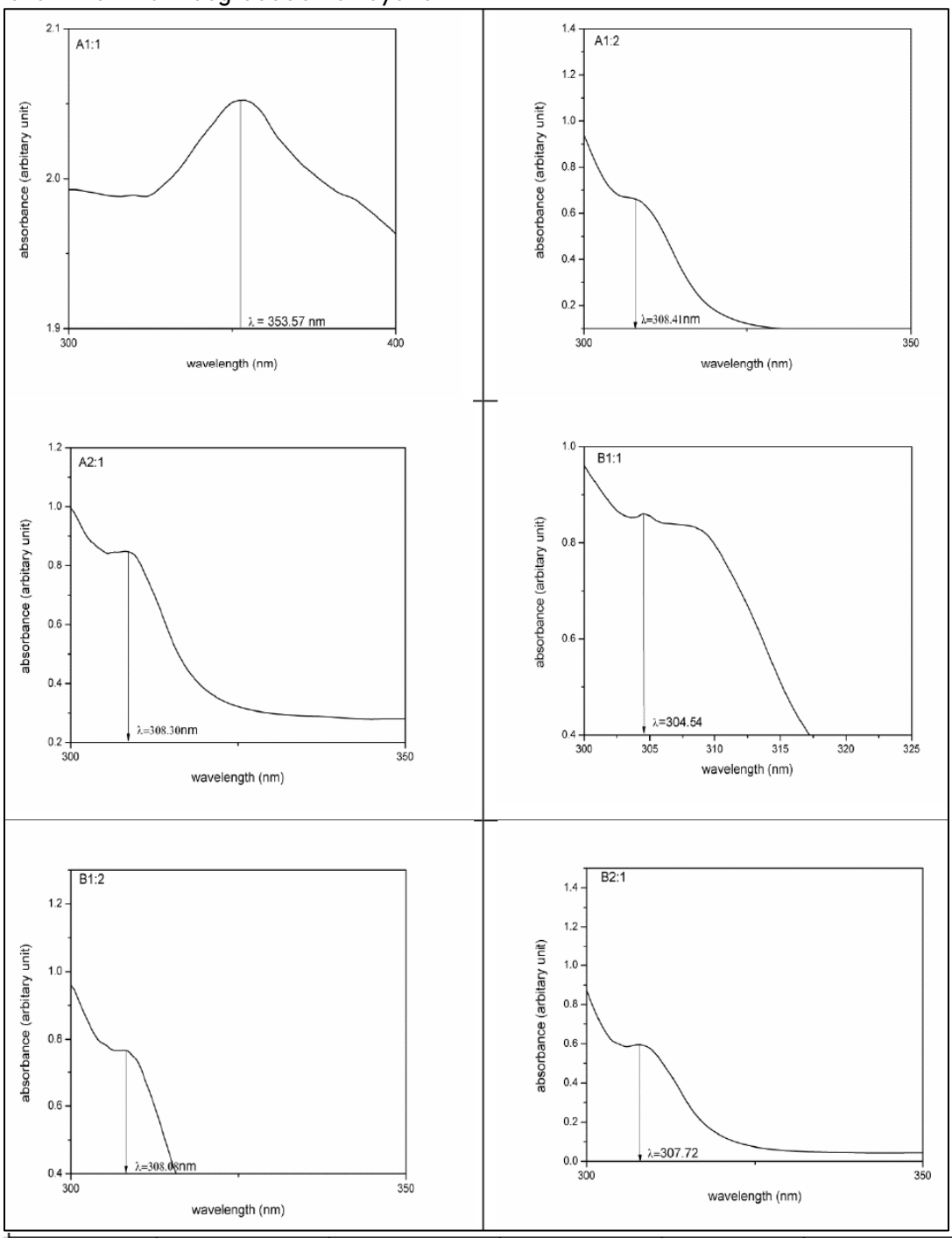

A 1:1	A 2:1	B 1:2	A 1:2	B 1:1	B 2:1
pH 3, 1:1 mole % of CdO and TiO2	pH 3, 2:1 mole % of CdO and TiO2	pH 13, 1:2 mole % of CdO and TiO2	pH 3, 1:2 mole % of CdO and TiO2	pH 13, 1:1 mole % of CdO and TiO2	pH 13, 2:1 mole % of CdO and TiO2

Fig. 3. UV-Vis transmittance spectra for all synthesized catalyst.

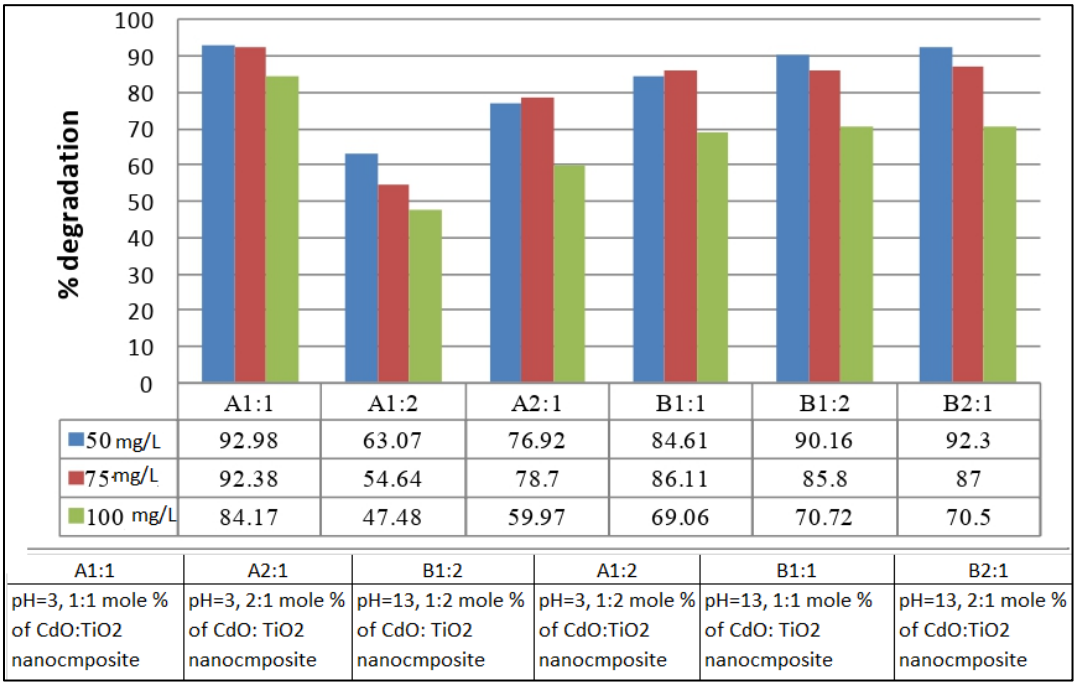

Fig. 4. Percentage degradation of RG-19 at various initial dye concentrations.

3.5. Effect of pH of dye solution

The pH of the dye sample is a significant factor in decomposition. It affects the surface charge of the semiconductor photocatalyst and thereby affects the transfer of electrons and the process of light-induced redox reaction. So it is important to know the pH effect on the light-induced decomposition of RG-19. The initial pH of the dye was 7.5. The pH effect was studied for pH-5 and pH-10, keeping the concentration of dye solution at 75 ppm and catalyst concentration 1 g/L at a constant value. The dependence of pH on the photocatalytic degradation of RG-19 is shown in Figure 5. The results indicate that pH-7.5 shows the maximum rate of degradation for all the synthesized catalysts. The results at pH-10 and pH-5 show a lower degradation rate than pH-7.5, which is in agreement with the results obtained by Chen et al. [26]. It is also reported that under acidic conditions, TiO_2 nanoparticles are agglomerated, and the surface available for dye adsorption is reduced, resulting in the reduction of the rate of degradation [27]. The photocatalyst A1:1 at pH-7.5 showed maximum degradation, i.e., 94.53 % after 180 minutes.

3.6. Effect of catalyst loading

The optimum catalyst loading was assessed by conducting three sets of experiments. These experiments were conducted by varying the amount of catalyst (0.5, 1, and 1.5 g/L). The initial dye content (75 ppm) and pH of the dye solution (pH-7.5) were kept constant. The effect of catalyst loading on the degradation of RG-19 is shown in Fig. 6. It was observed that the dye degrades faster with an increase in catalyst concentration from 0.5 g/L to 1 g/L. However, for the catalyst concentration of 1.5 g/L, there was an increase in turbidity. This resulted in a reduction in the light transmission through the solution, which in turn decreased the degradation rate. There was an increase in the number of active sites on the catalyst with an increase in catalyst concentration. This resulted in an increase in the number of hydroxyl and superoxide radicals, which were responsible for the rate of degradation. An increase in catalyst concentration above the optimum value resulted in a drop in the rate of degradation, owing to the rise in the solution's turbidity [28]. The aggregation of the catalyst occurred at a higher concentration of the catalyst, which reduced the surface area of the catalyst. And this resulted in a decrease in the rate of degradation. Catalyst A1:1 showed the maximum degradation at catalyst concentration 1 g/L, i.e., 94.53 %.

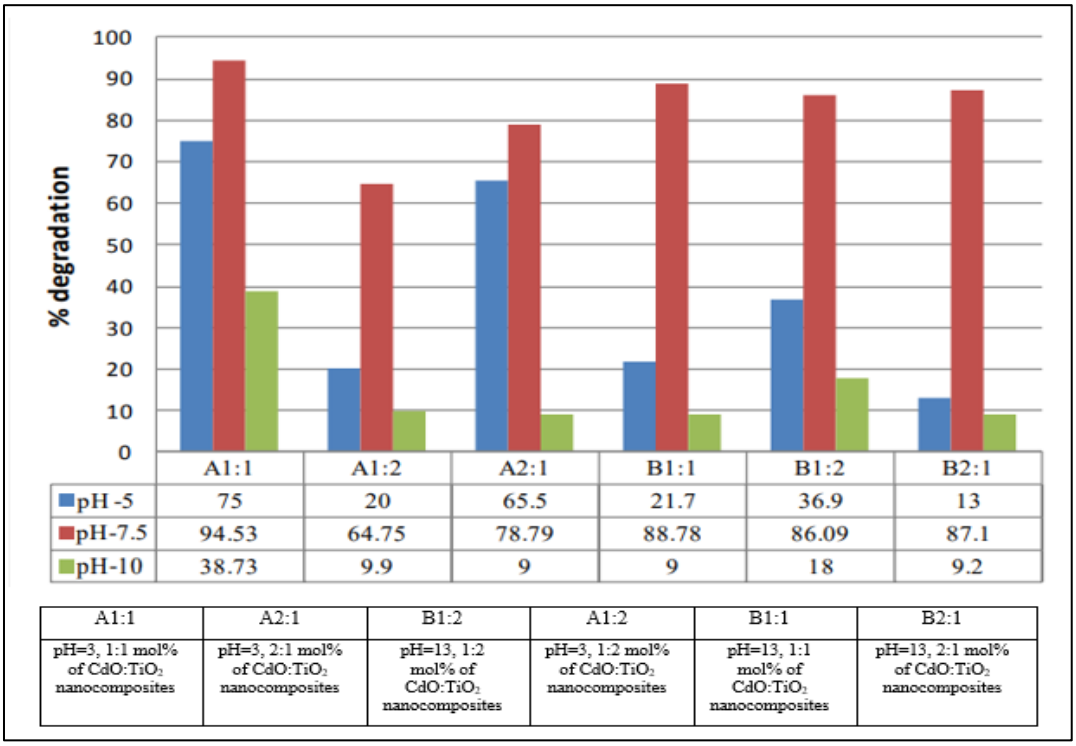

Fig. 5. Percentage degradation of RG-19 at various pH.

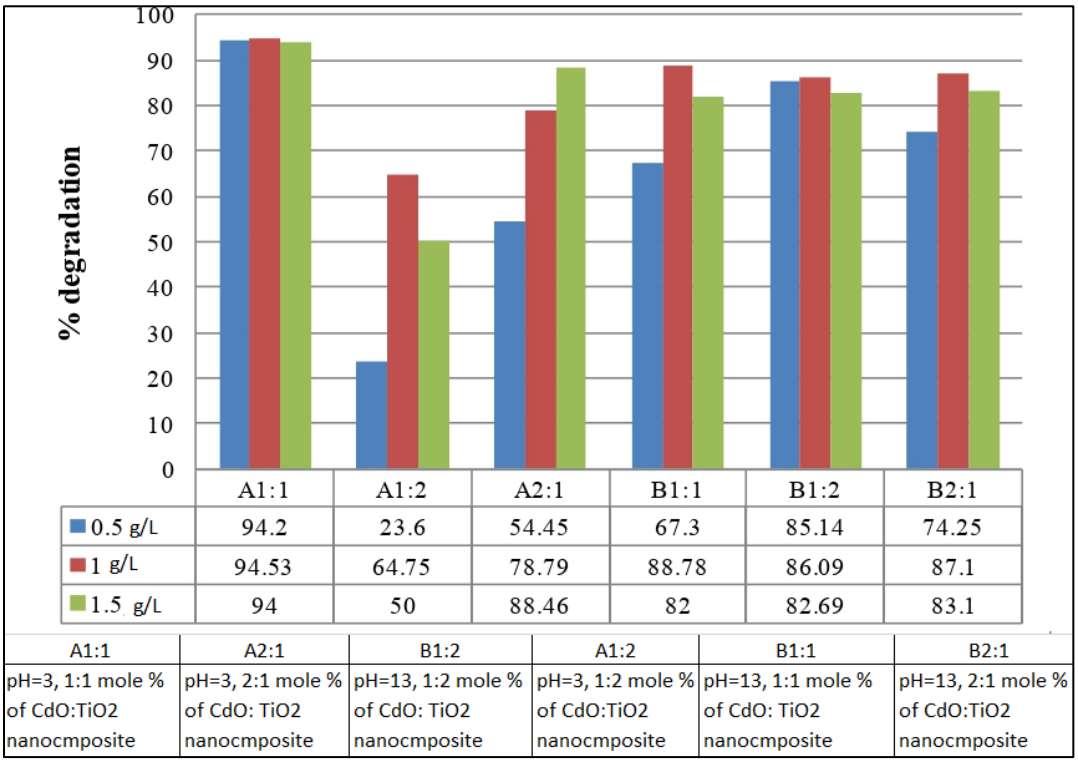

Fig. 6. Percentage degradation of RG-19 at different catalyst loading.

3.7. Effect of variation of molar ratio of CdO and TiO_2

Cadmium oxide has advantages such as high carrier concentration, high electrical conductivity, greater chemical stability, widespread availability, and high transparency in the visible range [29]. But at higher concentrations, due to the action of CdO as an

active site, the catalytic activity in the presence of CdO increases for the reduction of oxygen molecules by the electrons of the conduction band. So a decent combination of CdO with other catalysts is being explored. The effect of variation of molar ratio of CdO and TiO_2 in the catalysts on photocatalytic activity was observed from the degradation results of all catalysts. The A1:1 photocatalyst showed the maximum degradation of dye. The variation in the concentration of CdO and TiO_2 affected the particle size and band gap of nanoparticles. The larger particle size lowers the value of the band gap of the material, which ultimately affects photocatalytic activity [30,31]. Crystallite sizes, band gaps and % degradation for synthesized photocatalysts are depicted in Table 1. It was observed from the results (Table 1) that photocatalyst A1:1 had a lower band gap than the other photocatalyst.

Table 1. Crystallite size of the synthesized nanocomposites.

CdO-TiO_2 Catalyst	Crystallite size (nM)	Band gap (eV)	% Degradation
A 1:1	38.3	3.505	94.53
A 1:2	29.42	4.02	64.75
A 2:1	36.56	4.022	78.79
B 1:1	31.51	4.071	88.78
B 1:2	29.39	4.024	86.09
B 2:1	32.65	4.029	87.1

It has been reported that the lower the band gap, the higher the photocatalytic activity [32]. It was observed from optimized batch results that the photocatalyst synthesized at pH-3 showed the maximum degradation of dye. A similar result has been reported for the photocatalytic activity of the TiO_2 photocatalyst synthesized at pH-3 [33].

Conclusions

The photocatalytic degradation of pollutants is a promising method for effectively degrading dyes and other water pollutants [34]. Many investigators are exploring the synthesis and characterization of nanocomposites by various techniques [35]. In this study, the CdO-TiO_2 nanocomposites of different molar ratios (CdO: TiO2) were synthesized at pH-3 and pH-13 by the sol-gel method for application in photocatalytic degradation of azo dye (Reactive Green-19) under sunlight. Cadmium oxide has advantages like high carrier concentration, high electrical conductivity, greater chemical stability, widespread availability, and high transparency in the visible range [29]. But at higher concentrations, due to the action of CdO as an active site, the catalytic activity in the presence of CdO increases for the reduction of oxygen molecules by the electrons of the conduction band. So a decent combination of CdO with other catalysts is being explored. The changes in morphology, crystallinity, and optical properties due to change in the molar ratio of the precursor and pH variation were observed by FE-SEM, XRD, and UV-Vis spectrophotometer analysis. The FE-SEM images showed the change in morphology from a rod shape to a spherical shape for pH-3 and pH-13, respectively. The XRD analysis indicated a reduction in crystallinity as the pH changed from acidic to basic. Due to the change in the molar ratio of the precursor, the crystallite size was affected, and optical properties like absorption wavelength were also affected. The effect of variation in the operational parameters of photocatalysis, such as initial dye content, pH of dye solution, and catalyst loading, were observed and optimized as 75 ppm, pH-7.5, and 1gm/lit, respectively. Photocatalyst A1:1 showed maximum degradation (94.53%) of dye Reactive Green-19 in 180 minutes.

Acknowledgments

The authors express their gratitude to the Ministry of Human Resource Development initiative programme 'Technical Education Quality Improvement Program (TEQIP-II)' for providing financial assistance for this research. Also, the authors wish to thank the University Institute of Chemical Technology, Kavayitri Bahinabai Chaudhari North Maharashtra University Jalgaon, Maharashtra, India, and Gharda Institute of Technology, Lavel, Maharashtra, India.

References

[1] Yaseen, D.A., Scholz, M. (2019). Textile dye wastewater characteristics and constituents of synthetic effluents: a critical review. *Internatiomal. Journal of environmental. science and technology., 16,* 1193-1226..

[2] Zazouli, M. A., Azari, A., Dehghan, S., Razieh Salmani Malekkolae, R.S.(2016). Adsorption of methylene blue from aqueous solution onto activated carbons developed from eucalyptus

bark and *crataegus oxyacantha* core. *Water science and technology., 74(9),* 2021-2035.

[3] Sarkar, S., Banerjee, A., Halder, U., Biswas, R., Bandopadhyay, R. (2017). Degradation of synthetic azo dyes of textile industry: a sustainable approach using microbial enzymes. *Water conservation science and engineering*, *2*(4), 121-131.

[4] Saratale, R. G., Saratale, G. D., Chang, J. S., Govindwar, S. P. (2011). Bacterial decolorization and degradation of azo dyes: a review. *Journal of the Taiwan institute of chemical engineers*, *42*(1), 138-157.

[5] Moradi, M., Hosseini Sabzevari, M., Marahel, F., Shameli, A. (2021). Removal of reactive green KE-4BD and Congo red dyes in textile effluent by natural clinoptilolite particles on a biosorbent as a cheap and efficient adsorbent: experimental design and optimisation. *International journal of environmental analytical chemistry*, 1-19.

[6] Issabayeva, G., Hang, S. Y., Wong, M. C., Aroua, M. K.(2018). A review on the adsorption of phenols from wastewater onto diverse groups of adsorbents. *Reviews in chemical engineering, 34(6),* 855-873.

[7] Moazeni, M., Parastar, S., Mahdavi, M., Ebrahimi, A. (2020). Evaluation efficiency of Iranian natural zeolites and synthetic resin to removal of lead ions from aqueous solutions. *Applied water science*, *10*(2), 1-9.

[8] Bridges, L., Mohamed, R. A., Khan, N. A., Brusseau, M. L., Carroll, K. C. (2020). Comparison of manganese dioxide and permanganate as amendments with persulfate for aqueous 1, 4-dioxane oxidation. *Water*, *12*(11), 3061.

[9] Gautam, K., Kamsonlian, S., Kumar, S. (2020). Removal of Reactive Red 120 dye from wastewater using electrocoagulation: optimization using multivariate approach, economic analysis, and sludge characterization. *Separation science and technology*, *55*(18), 3412-3426.

[10] Schaefer, C. E., Yang, X., Pelz, O., Tsao, D. T., Streger, S. H., & Steffan, R. J. (2010). Aerobic biodegradation of iso-butanol and ethanol and their relative effects on BTEX biodegradation in aquifer materials. *Chemosphere*, *81*(9), 1104-1110.

[11] Haritash, A. K., Kaushik, C. P. (2009). Biodegradation aspects of polycyclic aromatic hydrocarbons (PAHs): a review. *Journal of hazardous materials*, *169*(1-3), 1-15.

[12] Loeb, S.K., Alvarez, P.J., Brame, J.A., Cates, E.L., Choi, W., Crittenden, J., Dionysiou, D.D., Li, Q., Li-Puma, G., Quan, X., Sedlak, D.L., Waite, T.D., Westerhoff, P., Kim, J. (2019). The technology horizon for photocatalytic water treatment: Sunrise or sunset?. *Environmental science and technology, 53(6),* 2937-2947.

[13] Lin, L., Jiang, W., Chen, L., Xu, P., Wang, H.(2020). Treatment of produced water with photocatalysis: Recent advances, affecting factors and future research prospects. *Catalysts, 10, 924*.

[14] Khataee, A. R. (2009). Photocatalytic removal of CI basic red 46 on immobilized TiO_2 nanoparticles: Artificial neural network modelling. *Environmental technology*, *30*(11), 1155-1168.

[15] Wang, Q., Zheng, K., Yu, H., Zhao, L., Zhu, X., Zhang, J.(2020). Laboratory experiment on the nano-TiO_2 photocatalytic degradation effect of road surface oil pollution. *Nanotechnology reviews, 9(1),* 922-933.

[16] Chebli, D., Fourcade, F., Brosillon, S., Nacef, S., Amrane, A. (2011). Integration of photocatalysis and biological treatment for azo dye removal–application to AR183. *Environmental technology*, *32*(5), 507-514.

[17] Pan, H., Heagy, M.D.(2020). Photons to formate: A review on photocatalytic reduction of CO_2 to formic acid. *Nanomaterials, 10(12),* 1-24.

[18] Konstantinou, I. K., Sakellarides, T. M., Sakkas, V. A., Albanis, T. A. (2001). Photocatalytic degradation of selected s-triazine herbicides and organophosphorus insecticides over aqueous TiO_2 suspensions. *Environmental science and technology*, *35*(2), 398-405

[19] Kwon, Y. T., Song, K. Y., Lee, W. I., Choi, G. J., Do, Y. R. (2000). Photocatalytic behavior of WO3-loaded TiO_2 in an oxidation reaction. *Journal of catalysis*, *191*(1), 192-199.

[20] Sakthivela, S., Neppolianb, B., Shankarb, M., Arabindoob, B.,Palanichamyb, M., Murugesan.

V. (2003). Solar photocatalytic degradation of azo dye: comparison of photocatalytic efficiency of ZnO and TiO_2. *Solar energy materials and Solar cells, 77(1),* 65–82.

[21] Kwon, Y. T., Song, K. Y., Lee, W. I., Choi, G. J., Do, Y. R. (2000). Photocatalytic behavior of WO3-loaded TiO_2 in an oxidation reaction. *Journal of catalysis*, *191*(1), 192-199.

[22] Nayak, J., Sahu, S. N., Kasuya, J., Nozaki, S. (2008). CdS–ZnO composite nanorods: synthesis, characterization and application for photocatalytic degradation of 3, 4-dihydroxy benzoic acid. *Applied surface science*, *254*(22), 7215-7218.

[23] Kumar, S., Selvakumar, M., Babu, G., Karuthapandian, S., Chattopadhyay, S. (2015). CdO nanospheres: Facile synthesis and bandgap modification for the superior photocatalytic activity. *Materials letters, 151,* 45-48.

[24] Huhtala, M., Heino, J., Casciari, D., de Luise, A., Johnson, M. S. (2005). Integrin evolution: insights from ascidian and teleost fish genomes. *Matrix biology*, *24*(2), 83-95.

[25] Konstantinou, I. K., Albanis, T. A. (2004). TiO_2-assisted photocatalytic degradation of azo dyes in aqueous solution: kinetic and mechanistic investigations: a review. *Applied catalysis B: Environmental, 49(1),* 1–14.

[26] Chen, L.C., Huang, C.M., and Tsai, F.R. (2007). Characterization and Photocatalytic Activity of K+-Doped TiO_2 Photocatalysts. *Journal of molecular catalysis A: Chemical, 265,* 133-140.

[27] Fox, M. A., Dulay, M. T. (1993). Heterogeneous photocatalysis. *Chemical reviews*, *93*(1), 341-357.

[28] Chakrabarti, S., Dutta, B. K. (2004). Photocatalytic degradation of model textile dyes in wastewater using ZnO as semiconductor catalyst. *Journal of hazardous materials*, *112*(3), 269-278.

[29] Zeid, E.F.A., Ibrahem, I.A., Ali, A.M., Walied A.A. Mohamed, W.A.A.(2019).The effect of CdO content on the crystal structure, surface morphology, optical properties and photocatalytic efficiency of p-NiO/n-CdO nanocomposite. *Results in physics*, *12*, 562-570.

[30] Pattabi, M., B, Saraswathi Amma. (2007). Effect of precursor concentration on the particle size of mercaptopropionic acid-capped CdS nanoparticles. *Journal of new materials for electrochemical systems*, *10*(1), 43-47.

[1] [31] Gupta, P., Ramrakhiani, M. (2009). Influence of the particle size on the optical properties of CdSe nanoparticles. *The open nanoscience journal*, *3*, 15-19.

[32] Nagaveni, K., Hegde, M. S., Ravishankar, N., Subbanna, G. N., Madras, G. (2004). Synthesis and structure of nanocrystalline TiO_2 with lower band gap showing high photocatalytic activity. *Langmuir*, *20*(7), 2900-2907.

[33] Huang, Y. U., Zheng, X., Zhongyi, Y. I. N., Feng, T. A. G., Beibei, F. A. N. G., Keshan, H. O. U. (2007). Preparation of nitrogen-doped TiO_2 nanoparticle catalyst and its catalytic activity under visible light. *Chinese journal of chemical engineering*, *15*(6), 802-807.

[34] Sahoo, S. K., Bhattacharya, S., Sahoo, N. K. (2020). Photocatalytic degradation of biological recalcitrant pollutants: a green chemistry approach. *Biointerface research in applied chemistry*, *10*(2), 5048-5060.

[35] Prabakar, A.C., Killivalavan, G., Sivakumar, D., Naidu, K.C.B., Sathyaseelan, B., Senthilnathan, K.,Baskaran, I., Manikandan, E., Rao, B.R., Sarma, M., et al. (2020). Structural, morphological, and magnetic properties of copper zinc cobalt ferrites systems nanocomposites. *Biointerface research in applied chemistry, 10(4)*, 6015-6019.